Mechanical behavior of carbon nanotubes in the rippled and buckled phase

H. Jackman,[1] P. Krakhmalev,[1] and K. Svensson[1, a)]
Department of Engineering and Physics, Karlstad University, SE-651 88 Karlstad, Sweden

(Dated: 7 March 2015)

We have studied the mechanical behavior of multi-walled carbon nanotubes for bending strains beyond the onset for rippling and buckling. We found a characteristic drop in the bending stiffness at the rippling and buckling onset and the relative retained stiffness was dependent on the nanotube dimensions and crystallinity. Thin tubes are more prone to buckle, where some lose all of their bending stiffness, while thicker tubes are more prone to ripple and on average retain about 20% of their bending stiffness. In defect rich tubes the bending stiffness is very low prior to rippling but these tubes retain up to 70% of their initial bending stiffness.

I. INTRODUCTION

Carbon nanotubes (CNTs) have a high mechanical stiffness, high electrical conductivity and are lightweight. These properties make CNTs ideal for high frequency nanoelectromechanical applications, such as nanorelays,[1,2] and nanoresonators.[3–5] Carbon nanotubes can be thought of as rolled up layers of graphene sheets, and the high in-plane stiffness of graphene gives the tubes an axial Young's modulus on the order of 1TPa.[6] In bending configurations, the high axial Young's modulus provides a high bending stiffness of the tubes, but only up to a critical point where tube walls start to ripple or buckle.[7–9] These deformations are similar to the behavior seen in macroscopic tubes (e.g. drinking straws) and it results in a significant reduction of the bending stiffness. At the very onset of rippling, the changes in morphology are very subtle,[10] and the onset is best detected by the abrupt drop in bending stiffness.[11] In the rippled and buckled phase there is also a concomitant reduction in the electrical conductivity.[12,13] Thus, if a nanorelay is operated into the rippled regime, it can cause problems both with stiction, due to a low restoring force, and a low electrical conductivity in the on-state. On the other hand, the deformation can be used for intentional modification of the electron transport, and it has enabled the construction of room-temperature single electron transistors.[14] As the rippling and buckling are reversible processes, they can also be exploited in energy absorbing materials.[15]

The rippling and buckling behavior of carbon nanotubes have been modelled extensively (for recent reviews see e.g. Ref. 16 and 17), but measurements are very challenging and the experimental characterizations are still at an infant stage.[16] The rippling pattern itself has been studied for embedded tubes[9,18] by using transmission electron microscopy (TEM), and force measurements have also been done for tubes supported on a substrate[19,20] by using atomic force microscopy (AFM). Ideally these two methods should be combined to enable studies of freestanding structures, and early attempts have been made by using different spring elements and post image analysis to estimate forces[21,22]. Only recently has the use of non-optical force sensors[23] provided a true joining of AFM with regular electron microscopy instruments, and this has enabled detailed studies of the critical bending-strain for buckling and rippling in carbon nanotubes.[11,24] These measurements have shown that both the initial stiffness and the rippling onset are very sensitive to the amount of defects in the nanotubes.[24] Tubes with a large defect density, grown by chemical vapour deposition (CVD) techniques, are much softer and ripple at larger strains compared to highly crystalline

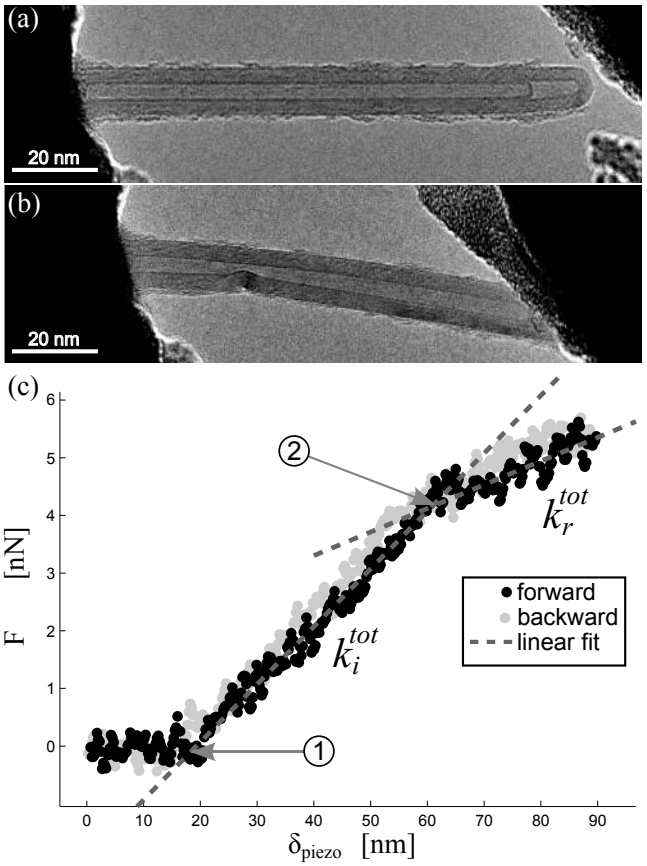

FIG. 1. TEM-images of a freestanding MWCNT, (a) when unloaded and (b) when bent. (c) A typical force (F) versus deflection (δ) curve obtained for a MWCNT.

a)Electronic mail: krister.s@kau.se

tubes grown by arc-discharge techniques. The rippling onset is also dependent on the number of walls in the tubes, as the inner tubes support the outermost tube, where the rippling first will appear. Such a supporting effect was first suggested from modeling.[25] The actual effect is larger than predicted though, and measurements have shown a variation by a factor of three in the critical strain, for CNTs with the same outer diameter.[24] The bending stiffness in the rippled phase has also been suggested to depend on the number of walls in a multi-walled carbon nanotube (MWCNT), but the modeling results vary from a rather weak,[26] to a very strong dependence.[27] There have not yet been any quantitative experimental data available, but the behavior will be important for the exploitation of strains beyond the initial linear regime in carbon nanotubes.

Here we report studies of the mechanical behavior of carbon nanotubes beyond the rippling and buckling onset. The tubes are mounted rigidly at one end while the free end is bent using a piezoresistive force sensor. The force response from each individual tube has been monitored continuously as a function of deflection, and provides a measure of the bending stiffness in the rippled phase. Beyond the critical strain, we find a near linear relation between force and deflection, albeit with a reduced bending stiffness compared to the initial stiffness. The relative retained stiffness has been analyzed with respect to a normalized thickness of the tubes. We find that highly crystalline tubes have a low relative retained stiffness after the rippling onset, while defects increase the retained stiffness, in reasonable agreement with previous modeling studies. In highly crystalline tubes, the number of walls will affect both the deformation mechanism and the relative retained stiffness.

II. EXPERIMENTAL

Measurements were performed on MWCNTs grown by CVD and the arc-discharge method. The CVD-grown MWCNTs were synthesized by Nanocyl (NC2100 and NC2101), and the tubes grown by the arc-discharge method were obtained from Professor Hui-Ming Cheng (at the Institute of Metal Research, Chinese Academy of Sciences). Arc-discharge grown CNTs have a much higher crystallinity compared to CVD-grown ones. This is fairly obvious from TEM images, where the walls of arc-discharge tubes are much straighter, but it is difficult to quantify the amount of defects.[28] By using both materials we are able to observe the influence of defects on the material properties qualitatively.

Individual MWCNTs were pushed against a piezoresistive force sensor, in a cantilever-to-cantilever fashion, inside a TEM and inside a scanning electron microscope (SEM). The in situ instrument, enabling manipulation and force measurements, was obtained from Nanofactory Instruments AB for the TEM and custom made for the SEM using the same type of manipulator and force detection system. Measurements on tubes grown by arc-discharge where performed inside a JEOL (JEM 2100) TEM, equipped with a LaB_6 cathode and a digital camera from Gatan (SC1000 Orius). The sample was inserted and left in the chamber for at least 10 hours before the measurements, reaching a pressure of about 7×10^{-8} Torr (with the use of a liquid nitrogen cooling trap). This was done in order to minimize any risk of amorphous carbon build up when exposing the carbon nanotubes to the electron beam. The acceleration voltage was set at 80 kV, which is below the threshold for knock-on damage in graphene.[29] To further reduce the risk for beam induced effects, the electron beam was deflected away from the sample and force sensor during the force measurements since damages can occur even at 80kV in strained sp^2-carbon bonds,[30] due to ionization effects.[31]

Measurements on the CVD-grown tubes were performed inside a LEO 1530 FEG-SEM, operated at an acceleration voltage of 12 kV and a chamber pressure of about 5×10^{-7} Torr. The beam was deflected away from sample and sensor during measurements, in order to avoid beam induced effects. The experimental set-up and further details on how the measurements were performed, and calibrated, have been described elsewhere.[11,24]

III. DROP IN BENDING STIFFNESS

A typical measurement is shown in Fig. 1, where a MWCNT has been imaged (a) before, and (b) during force measurements. Fig. 1 (c) shows a typical force, F, versus deflection, δ, curve, where at first the force is zero until the CNT comes in contact with the force sensor at point 1 indicated in the figure. From this point and on the force increases linearly with the deflection, having an initial spring constant of k_i^{tot}, until at point 2 where the stiffness abruptly decreases. After point 2 the force continues to increase approximately linearly but with a lower rippling phase spring constant k_r^{tot}. The measured spring constants, $k_{i,r}^{tot}$, are related to the spring constants of the sensor, k^{sens}, and that of the CNT, $k_{i,r}$, through:

$$k_{i,r} = \frac{k^{sens} k_{i,r}^{tot}}{k^{sens} - k_{i,r}^{tot}} \tag{1}$$

By assuming the CNTs to be cantilevered beams with a hollow circular cross-section, the Young's modulus can be obtained using the spring constants and the dimensions of the CNT.

$$E_{i,r} = \frac{64}{3\pi} \frac{k_{i,r} l^3}{(d_o^4 - d_i^4)} \tag{2}$$

Where l is the length, and d_o and d_i are the outer and inner diameter of the CNT. The rippling phase Young's modulus, E_r, should only be seen as an apparent parameter, as the cross-section of the CNT is altered after the rippling onset. Further on, E_r is only used in comparison with E_i and not as an absolute measure.

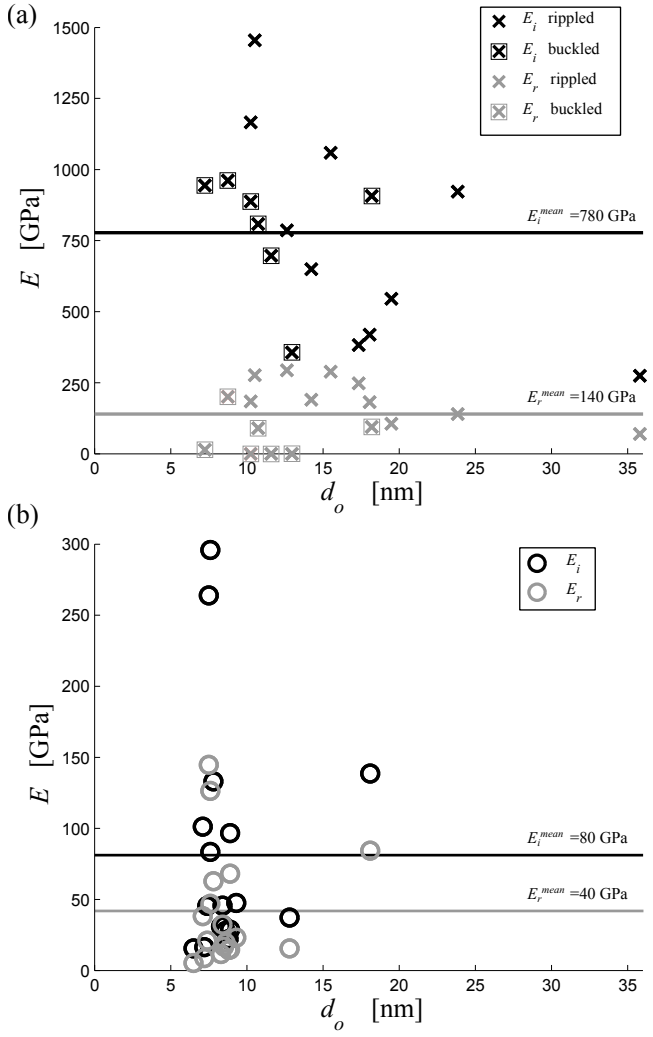

FIG. 2. Young's modulus (E) vs. outer diameter (d_o) before and after the rippling onset, for (a) tubes grown by arc-discharge and (b) CVD-grown tubes. The horizontal lines indicate the average values for each phase.

Since the CVD-grown tubes were measured inside a SEM, the inner diameter could not easily be measured. However most tubes had a large normalized thickness ($t_N = \frac{d_o - d_i}{d_o} > 0.5$) making the effect from the inner diameter on E_i negligible.[11] To get a good accuracy in measuring the outer diameter, the second derivative of the integrated intensity profile was used.[32] Multiplying Eq. 2 with the ratio k_r/k_i yields the Young's modulus after the rippling onset. The initial linear regime and the very onset of localized deformations have been analyzed in detail before.[11,24] Here we are focussing on the behavior after the very onset of buckling and rippling. This is most often referred to as a non-linear regime, but this can be a little misleading as we find an approximately linear dependence also above the critical strain. Instead we here refer to this strain regime as a rippled phase of the nanotube. To analyze the mechanical behavior in the rippled phase, we have plotted Young's modulus before, E_i, and after, E_r, the rippling onset in Fig. 2, for (a) tubes grown by arc-discharge and (b) CVD-grown tubes. The arc-discharge tubes are, to begin with, much stiffer than the CVD tubes as a result of their higher degree of crystallinity.[24] Moreover, the relative drop in E for the arc-discharge tubes are much larger than the drop for the CVD tubes as is shown in Fig. 2. For the tubes grown by arc-discharge we have also distinguished between the tubes that buckle and those that ripple. Here we define buckling as a deformation where only one kink were observed, as is seen in Fig. 1 (b). Deformation where more than one kink were observed is referred to as rippling. From this definition it can be seen, in Fig. 2 (a), that the Young's modulus after the critical strain is much smaller for the buckled tubes compared to the rippled tubes. Some buckled tubes have even lost all their bending stiffness, as one might expect for thin walled tubes.[8,33]

From Fig. 2 there seems to be a trend for CNTs with a large E_i, i.e. tubes with a high crystallinity, to have a larger drop in their stiffness compared to tubes with a smaller E_i. To investigate this further, we have plotted the relative retained stiffness, k_r/k_i, versus the initial Young's modulus, E_i, in Fig. 3. In this plot there is a general trend that tubes with a high crystallinity (high E_i) have a smaller relative retained stiffness, compared to defect rich ones (low E_i). This also indicates that some of the tubes grown by arc-discharge are not defect-free (i.e. tubes with $E_i < 500$ GPa).

The smaller relative reduction in the bending stiffness for CVD-grown tubes is consistent with simulations where it was found that the existence of interlayer bridges in MWCNTs will give a higher post-rippling stiffness.[34] CVD-grown tubes contain many types of defects, and these might have different effects on the mechanical properties. Vacancies might contribute mainly to a reduced axial stiffness, while inter-wall bridges may improve the post-rippling stiffness. It is worth noting that although the relative retained stiffness is higher for CVD-grown tubes, the value of E_r is still lower in these tubes compared to the ones grown by arc discharge.

In Fig. 4 the relative retained stiffness, k_r/k_i, is plotted versus the normalized thickness, t_N. Here we have only included data-points from tubes with $E_i > 500$ GPa, in order to ensure a high crystallinity of the tubes. One can see that thin tubes (with $t_N < 0.6$) preferably buckle while for thick tubes (with $t_N > 0.8$) there is only rippling deformation. There is however a fairly large range in the t_N values where tubes can both ripple or buckle, which means that the deformation mechanism is not solely determined by the value of t_N. Our definition of rippling and buckling is also rather crude due to the bending geometry with cantilevered tubes, as the bending moment varies linearly along the length of the tubes and has a maximum at the attachment point. Hence, the rippling deformations will have tendency to become localized near the attachment point at low loads, and the distinction between the two deformation mechanisms is

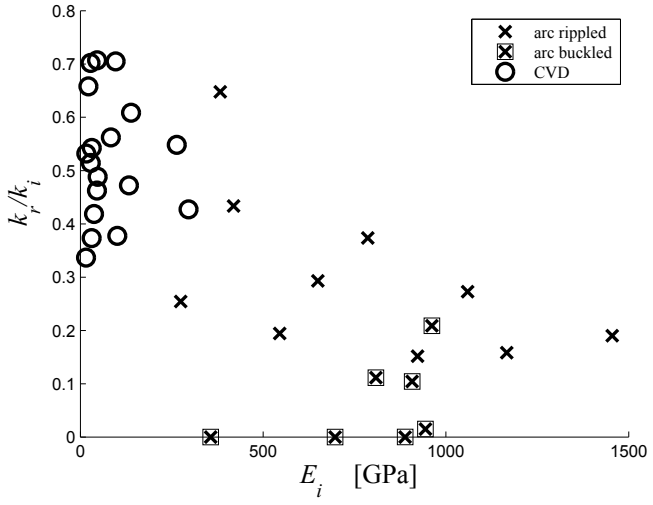

FIG. 3. Retained relative bending stiffness, k_r/k_i, versus Young's modulus in the initial linear phase, E_i.

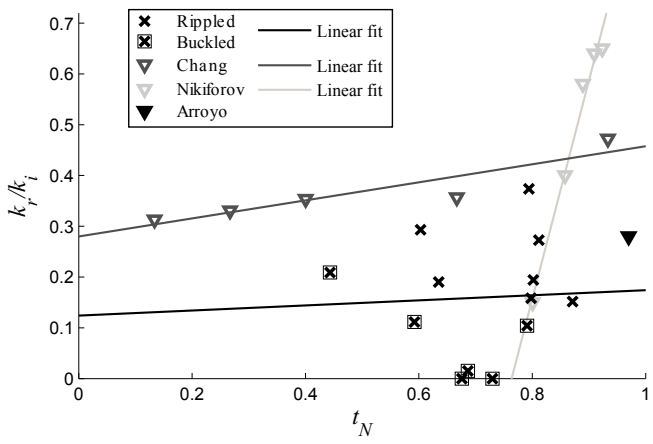

FIG. 4. Retained relative bending stiffness, k_r/k_i, versus normalized wall thickness, t_N, for arc-discharge grown tubes (crosses). Triangles indicate results from modelling, Nikiforov,[27] Chang,[26] and Arroyo.[10]

not as well defined as in modeling studies using a constant bending moment.[26,27]

A linear fit to all the experimental data points in Fig. 4 (rippled and buckled), results in a weakly increasing function, with values of k_r/k_i ranging from about 0.12 to 0.17 (as t_N goes from 0 to 1). This behavior is similar to what was found from modeling in Ref. 26, where a weak dependence of k_r/k_i on t_N was found, but it is in sharp contrast to the strong dependence found from modeling in Ref. 27, as illustrated in Fig. 4. In both these modeling studies the application of the load differs from our experimental work, as the models used an evenly distributed bending moment along the MWCNTs. In Ref. 10 a cantilevered MWCNT was modelled and a value for k_r/k_i of about 0.23 was obtained, in close agreement with the values obtained for rippled tubes in this study.

IV. GRADUAL DEFORMATION

For short and thick tubes, i.e. with small l and large d_o and t_N, the $F-\delta$ curves reveal some interesting features, as can be seen in Fig. 5. At point 1 there is a sudden drop in stiffness, as most simulations have predicted. In contrast to most simulations, a drop in the force is observed at point 2. After this drop the force continues to increase linearly, albeit with a slightly lower stiffness than between point 1 and 2. Upon retraction the $F-\delta$ curve is linear until point 3 where there is a small increase in the force as the tube returns to the initial linear response. This behavior is reproducible during cyclic motion, indicative of purely elastic deformations. The drop in force at point 2, which is beyond the critical strain, suggests that there is more than one critical point where the mechanical behavior is changed. Due to the high sensitivity of strained sp^2-carbon bonds to electron irradiation, we have not attempted any further TEM analysis of the rippling regime.

Simulations of MWCNTs have found a similar abrupt drop in the force,[26] but the mechanism behind the drop was not discussed, and no cyclic loading was studied. Modeling of SWNTs have predicted a similar hysteretic behavior.[33] The effect was attributed to a gradual buckling (during loading), combined with van der Waals interactions between opposing walls in the fully collapsed tube, thus delaying the relaxation point during unloading. The tubes where we have clearly observed this behavior all have large t_N, and we suggest that at point 1 the outermost wall ripples and between point 1 and 2 the rippling deformation spreads to the inner walls of the CNT. Finally at point 2 the innermost wall ripples and there is a drop in the force. A similar behavior is likely present in all tubes, but tubes with a smaller t_N will display a shorter distance between point 1 and 2. The behavior is then easily obscured, especially in measurements having a low signal-to-noise ratio.

Going back to Fig. 1 (c), there seems to be a drop in the force around the critical strain for rippling, but the signal-to-noise ratio prohibits this from showing conclusively. Also the extent of the regime just after the change in bending stiffness and before the drop in force is much smaller, compared to Fig. 5, as a result of the smaller value of t_N.

The behavior described above will give rise to hysteretic damping, and affect the performance of nanorelays and nanoresonators if these are oscillated beyond the critical strain for rippling, i.e. beyond point 2 in Fig. 5.

V. CONCLUSIONS

We find that the relative retained stiffness in the rippled and buckled state is highly dependent on the crystallinity. For highly crystalline tubes the relative retained stiffness varies between 0 and about 30%, depending mostly on the deformation mechanism. Thin tubes,

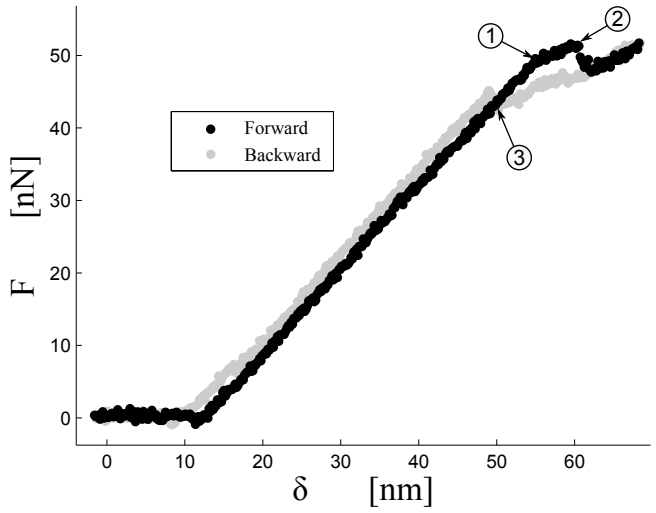

FIG. 5. Force, F, versus deflection, δ, for a short tube with a large normalized thickness, t_N, value. The arrows indicate three transition points in the mechanical behavior.

having small t_N, had a higher tendency to buckle and lose much of their bending stiffness. Thicker tubes had a higher tendency to ripple and their relative retained bending stiffness did not vary appreciably with t_N. For $t_N \geq 0.8$ we only observed rippling and the tubes had an averaged retained stiffness of about 20%.

For applications where the initial stiffness is less important, the use of CVD grown tubes can enable a retained stiffness of about 35-70%.

Our results show that one should carefully choose the operating range and growth technique depending on the application.

ACKNOWLEDGEMENTS

Financial support from The Swedish Research Council (project number 2010-4324) is gratefully acknowledged.

[1]S. Axelsson, E. E. B. Campbell, L. M. Jonsson, J. Kinaret, S. W. Lee, Y. W. Park, and M. Sveningsson, New J. Phys. **7**, 245 (2005).
[2]Y. A. Tarakanov and J. M. Kinaret, Nano Lett. **7**, 2291 (2007).
[3]V. Sazonova, Y. Yaish, H. Üstünel, D. Roundy, T. A. Arias, and P. L. McEuen, Nature **431**, 284 (2004).
[4]B. Lassagne, Y. Tarakanov, J. Kinaret, D. Garcia-Sanchez, and A. Bachtold, Science **325**, 1107 (2009).
[5]J. Chaste, A. Eichler, J. Moser, G. Ceballos, R. Rurali, and A. Bachtold, Nat. Nanotechnol. **7**, 301 (2012).
[6]M. S. Dresselhaus, G. Dresselhaus, J. C. Charlier, and E. Hernández, Philos. T. Roy. Soc. A **362**, 2065 (2004).
[7]S. Iijima, C. Brabec, A. Maiti, and J. Bernholc, J. Chem. Phys. **104**, 2089 (1996).
[8]B. I. Yakobson, C. J. Brabec, and J. Bernholc, Phys. Rev. Lett. **76**, 2511 (1996).
[9]O. Lourie, D. M. Cox, and H. D. Wagner, Phys. Rev. Lett. **81**, 1638 (1998).
[10]M. Arroyo and I. Arias, J. Mech. Phys. Solids **56**, 1224 (2008).
[11]H. Jackman, P. Krakhmalev, and K. Svensson, Appl. Phys. Lett. **98**, 183104 (2011).
[12]A. Rochefort, P. Avouris, F. Lesage and D. R. Salahub, Phys. Rev. B **60**, 824 (1999).
[13]A. A. Farajian, B. I. Yakobson, H. Mizuseki, and Y. Kawazoe, Phys. Rev. B **67**, 205423 (2003).
[14]H. W. C. Postma, T. Teepen, Z. Yao, M. Grifoni, and C. Dekker, Science **293**, 76 (2001).
[15]A. Misra, J. R. Raney, L. De Nardo, A. E. Craig, and C. Daraio, ACS Nano **5**, 7713 (2011).
[16]C. M. Wang, Y. Y. Zhang, Y. Xiang, and J. N. Reddy, Appl. Mech. Rev. **63**, 030804 (2010).
[17]H. Shima, Materials **5**, 47 (2012).
[18]C. Bower, R. Rosen, and L. Jin, Appl. Phys. Lett. **74**, 3317 (1999).
[19]M. R. Falvo, G. J. Clary, R. M. Taylor, V. Chi, F. P. Brooks, S. Washburn, and R. Superfine, Nature **389**, 582 (1997).
[20]X. Duan, C. Tang, J. Zhang, W. Guo, Z. Liu, and Zhongfan, Nano Lett. **7**, 143 (2007).
[21]T. Kuzumaki, and Y. Mitsuda, Jap. J. Appl. Phys. **45**, 364 (2006).
[22]K. Jensen, W. Mickelson, A. Kis, and A. Zettl, Phys. Rev. B, **76**, 1 (2007).
[23]A. Nafari, D. Karlen, C. Rusu, K. Svensson, H. Olin, and P. Enoksson, J. Microelectromech. Syst. **17**, 328 (2008).
[24]H. Jackman, P. Krakhmalev, and K. Svensson, Appl. Phys. Lett. **104**, 021910 (2014).
[25]T. Chang, W. Guo, and X. Guo, Phys. Rev. B **72**, 064101 (2005).
[26]T. Chang and J. Hou, J. Appl. Phys. **100**, 114327 (2006).
[27]I. Nikiforov, D.-B. Zhang, R. D. James, and T. Dumitrica, Appl. Phys. Lett. **96**, 123107 (2010).
[28]J. H. Lehman, M. Terrones, E. Mansfield, K. E. Hurst, and V. Meunier, Carbon **49**, 2581 (2011).
[29]J. C. Meyer, F. Eder, S. Kurasch, V. Skakalova, J. Kotakoski, H. J. Park, S. Roth, A. Chuvilin, S. Eyhusen, G. Benner, A. V. Krasheninnikov, and U. Kaiser, Phys. Rev. Lett. **108**, 196102 (2012).
[30]J. H. Warner, F. Schffel, G. Zhong, M. H. Rmmeli, B. Bchner, J. Robertson, and G. A. D. Briggs, ACS nano, **3**, 1557 (2009).
[31]K. Kim, V. I. Artyukhov, W. Regan, Y. Liu, M. F. Crommie, B. I. Yakobsson, and A. Zettl, Nano Lett. **12** 293 (2012).
[32]H. Jackman, P. Krakhmalev, and K. Svensson, Ultramicroscopy **124**, 35 (2013).
[33]A. Kutana and K. P. Giapis, Phys. Rev. Lett. **97** 245501 (2006).
[34]X. Huang, H. Yuan, W. Liang, and S. Zhang, J. Mech. Phys. Solids **58**, 1847 (2010) .